

## Physicochemical Characterization and Dissolution Properties of CS-891 with Different Crystallinity

Woo-Young Lee<sup>†</sup>, Byoung-Woo Park and Yong-Sun Park

Pharmaceutical Development Labs, SamChunDang Pharma. Co., LTD., HyangNam 904-1, Korea

(Received June 16, 2005 · Accepted July 11, 2005)

**ABSTRACT** – Ground CS-891 (N-[1-(4-methoxyphenyl)-1-methylethyl]-3-oxo-4-aza-5a-androst-1-ene-17 $\beta$ -carboxamide) of poorly water soluble drug was obtained using a Heiko Seisakusho model TI-100 vibration mill, and samples with different crystallinity were prepared at mixture ratios of 10:0, 7:3, 5:5, 3:7 and 0:10 (intact:ground CS-891). Physicochemical characterizations were obtained using qualitative and quantitative X-ray diffractometry, different scanning calorimetry (DSC), scanning electron microscopy (SEM), Quantasorb surface area analyzer, and controlled atmosphere microbalance. With increase of amorphous CS-891 in mixture ratios, the intensities of X-ray diffraction peaks of crystalline CS-891 were decreased, whereas surface area, water absorption, and exothermic peaks in DSC were increased. The apparent solubility of ground CS-891 was 4.4  $\mu\text{g/ml}$  and the solubility of intact CS-891 was 3.1  $\mu\text{g/ml}$  at 37 $\pm$ 1 $^{\circ}\text{C}$ . The apparent precipitation rates of CS-891 in a supersaturated solution during the solubility test were increased with an increase of amorphous CS-891, and a crystalline form of CS-891 transformed from amorphous CS-891 after the solubility test was found by X-ray diffraction analysis, DSC and SEM. The dissolution profiles of CS-891 with different crystallinity at 37 $\pm$ 1 $^{\circ}\text{C}$  by the USP paddle method were investigated, and the apparent dissolution rate constant of ground CS-891 was about 5.9-fold higher than that of intact CS-891. A linear relationships between the crystallinity of CS-891 and the apparent dissolution rate constant ( $r > 0.96$ ) were obtained.

**Key words** – CS-891, Crystallinity, Dissolution rate, Solubility

N-[1-(4-methoxyphenyl)-1-methylethyl]-3-oxo-4-aza-5a-androst-1-ene-17 $\beta$ -carboxamide (CS-891), which was developed and patented by Sankyo Co. LTD., is a potent 5 $\alpha$ -reductase inhibitor that has shown limited success in men treated for benign prostatic hyperplasia (success was defined as decrease in the symptoms associated with urinary tract obstruction, and as increases in the urinary flow rate). 5 $\alpha$ -reductase is necessary for the prostatic conversion of testosterone to dihydrotestosterone (DHT), the specific steroid that stimulates prostate transitional zone growth.<sup>1-3)</sup> CS-891 lowers levels of DHT, which is a major cause of prostate growth, and leads to shrinkage of the enlarged prostate gland in most men.<sup>4)</sup> This can lead to gradual improvement in urine flow and symptoms over the next several months. The chemical structure, as shown in Figure 1, is analogous to the aza-steroid finasteride. CS-891 is freely soluble in chloroform, ethanol and methanol, and soluble in acetone and acetonitrile, but the drug is poorly soluble in water. Crystallinity is an important parameter which affects the pharmaceutical properties of drug, such as dissolution rate, solubility, bioavailability, chemical stability,

tableting compression behavior and others.<sup>5-11)</sup> In this paper, we investigated the physicochemical properties of CS-891 with different crystallinity using X-ray diffractometry, DSC, SEM, Quantasorb surface area analyzer, and controlled atmosphere microbalance. The relationships between the crystallinity of CS-891 and the apparent dissolution rate constant, and the water sorption isotherms were also studied as well as the solubilities of these.

### Experimental

#### Materials

CS-891 was provided by Sankyo Co., LTD. High performance liquid chromatography (HPLC)-grade acetonitrile,

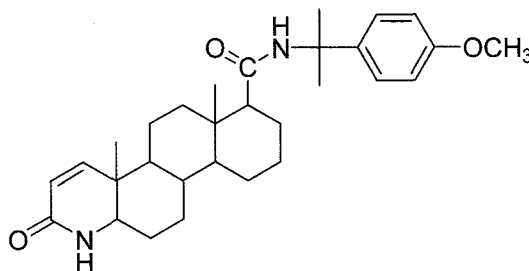


Figure 1—Chemical structure of CS-891.

<sup>†</sup>본 논문에 관한 문의는 이 저자에게로  
Tel : 031)353-1729, E-mail : pwylee@scd.co.kr

monobasic sodium phosphate, and dibasic sodium phosphate were purchased from VWR Scientific (West Chester, PA, USA). All other reagents and solvents used were of analytical grade.

#### Preparation of CS-891 with Different Crystallinity

CS-891 with different crystallinity was prepared at mixture ratios of 10:0 (ICS100), 7:3 (ICS70), 5:5 (ICS50), 3:7 (ICS30) and 0:10 (ICS0) (intact:ground CS-891), and stored in refrigerator at 4°C. CS-891 of 3 g was ground using a vibration mill (Heiko Seisakusho model TI-100)<sup>12-13)</sup> equipped with a rod and a zirconia cell for 30 min without temperature control. The ground CS-891 was withdrawn from the zirconia cell and passed through a 80 mesh screen.

#### Powder X-ray Diffraction (XRD) Analysis

All X-ray diffraction profiles were taken at room temperature with an X-ray diffractometry (RINT 2200 diffractometry). The operation conditions were as follows: target, Cu; filter, Ni; voltage 40 kV, current, 40 mA; receiving slit, 0.15 mm; time constant, 1s; counting range, 1k count per second (Kcps); scanning speed, 4° 2 $\theta$ /min.

#### Thermal Analysis

Thermal analysis of CS-891 was performed using DSC (Rigaku Thermo Plus, DSC 8230L). Samples were placed (5-10 mg) on an open sample pan and scanned at a rate 4°C or 10°C/min from 30 to 300°C under a flow of nitrogen gas.

#### Specific Surface Area

About 300-500 mg of each sample accurately weighed into the sample cell of a surface analyzer (Quantasorb Sorption System, Quantachrome). The specific surface area was determined by the multipoint BET method.<sup>14)</sup>

#### The Controlled Atmosphere Microbalance

The water sorption isotherms were determined by the gravimetric method at 35°C with a controlled RH glass vacuum assembly with a Vapor Sorption Analyzer (SGA-100, VTI Co.). A sample of ~7 mg was suspended in the isothermal chamber, exposed to RH from 2.5% to 95%, and monitored the water uptake gravimetrically.

#### Solubility Measurement

An excess 60 mg of intact CS-891 was placed into a 50 ml glass containers in 30 ml of purified water. All of these were closed with stopper, and the suspension was gently stirred for 24 hours at 37±1°C.<sup>15-16)</sup> After equilibrium, the suspensions

was quickly filtered through a 0.45  $\mu$ m membrane filter (PVDF; Whatman) and then diluted 2-fold with a methanol. The concentration of CS-891 dissolved was determined by HPLC.

The apparent solubility measurement of CS-891 with different crystallinity was carried out by the USP paddle method for dissolution testing.<sup>17)</sup> An excess 150 mg of each sample was put into 300 ml of purified water at 37±1°C, and the rotation speed of paddle was 200 rpm. The concentration of CS-891 dissolved was determined periodically with a ultraviolet spectrophotometer connected with a flow cell system at 225 and 240 nm as an appropriate times.

#### Dissolution Studies

The Dissolution experiment was also performed using the USP paddle method. Each of 10 mg of CS-891 with different crystallinity was carefully placed into 300 ml of purified water of dissolution medium. The dissolution medium was maintained at a temperature of 37±1°C, and the stirring speed used was 200 rpm. The concentration of CS-891 dissolved was measured periodically with a ultraviolet spectrometer connected with a flow cell system at 225 and 240 nm as an appropriated times.

## Results and Discussion

#### The XRD and Thermal Behavior of CS-891

The powder XRD patterns of ICS100, ICS70, ICS50, ICS30 and ICS0 are shown in Figure 2. The intensities of the crystalline peaks of CS-891 decreased with an increase of amorphous CS-891 in mixture ratios, and the values of crystallinity of ICS100, ICS70, ICS50, ICS30 and ICS0 were calculated by peak area method, modified Hermans method,<sup>18)</sup> and were 70, 46, 35, 22 and 4%, respectively.

Figure 3 shows the DSC thermograms of ICS100, ICS70, ICS50, ICS30 and ICS0. The melting point of each sample appeared at 248°C on the DSC curves of each sample. The thermograms of ICS100, ICS70, ICS50, ICS30 and ICS0 showed an exothermic peak but only exhibited an endothermic peak in case of ICS100. The small endotherm on the DSC curve of ICS100 might be due to the polymorph transformation from ICS100 to another crystal form. Table I shows the heat of crystallization ( $H_c$ ) and the heat of fusion ( $H_f$ ) of ICS100 and ICS0 were 5.084, -95.256 and 41.179, -86.117 Jg<sup>-1</sup>.

#### Surface Area and Water Sorption Isotherm

Table II shows the specific areas of ICS100, ICS70, ICS50, ICS30 and ICS0 were 1.244, 3.134, 4.882, 5.528 and 5.594 m<sup>2</sup>/

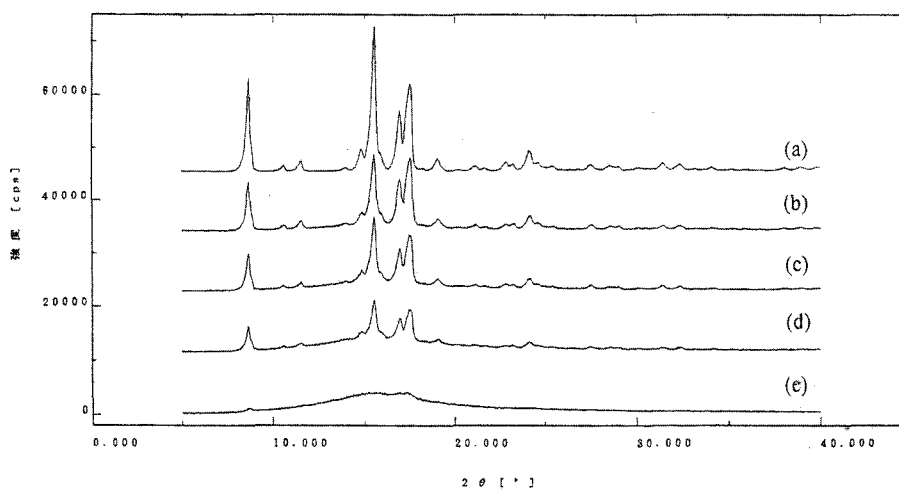


**Figure 2**–Powder X-ray diffraction patterns of ICS100, ICS70, ICS50, ICS30 and ICS0. (a) ICS100, (b) ICS70, (c) ICS 50, (d) ICS30, (e) ICS0.

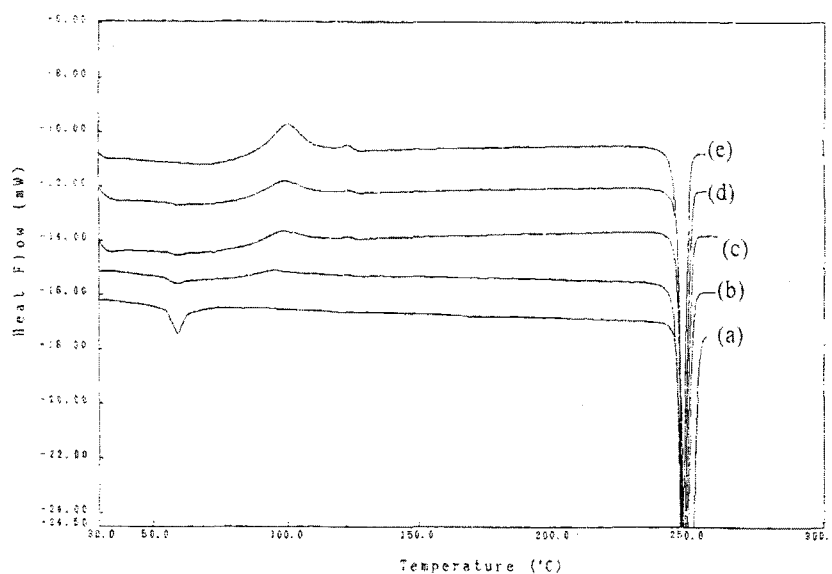


**Figure 3**–DSC thermograms of ICS100, ICS70, ICS50, ICS30 and ICS0. (a) ICS100, (b) ICS70, (c) ICS 50, (d) ICS30, (e) ICS0.

**Table I**–Heat of Crystallization and Heat of Fusion in DSC for CS-891 with Different Crystallinity

Samples	Crystallinity (%)	Heat of Crystallization ( $\Delta H_c, \text{Jg}^{-1}$ )	Heat of Fusion ( $\Delta H_f, \text{Jg}^{-1}$ )	$ \Delta H_c/\Delta H_f $
ICS100	70	5.084	-95.256	0.053
ICS70	46	8.157	-95.183	0.086
ICS50	35	21.865	-94.617	0.231
ICS30	22	26.317	-89.101	0.295
ICS0	4	41.179	-86.117	0.478

**Table II**–Crystallinity, Solubility, Apparent Dissolution Rate (ADR) Constant and Surface Area of CS-891 With Different Crystallinity

Samples	Crystallinity (%)	Solubility ( $\mu\text{g/ml}$ )	ADR Constant	Surface Area ( $\text{m}^2/\text{g}$ )
ICS100	70	3.1	0.451	1.244
ICS70	46	4.2*	1.713	3.134
ICS50	35	3.9*	2.054	4.882
ICS30	22	4.0*	2.512	5.528
ICS0	4	4.4*	2.657	5.594

\*: Apparent solubility.

g, and the specific surface areas were increased with a decrease of crystalline CS-891. The water vapor sorption isotherms for CS-891 with different crystallinity at 35°C are given in Figure

4. The isotherm for ground CS-891 showed a significant sorption of water, whereas intact CS-891 exhibited negligible sorp-

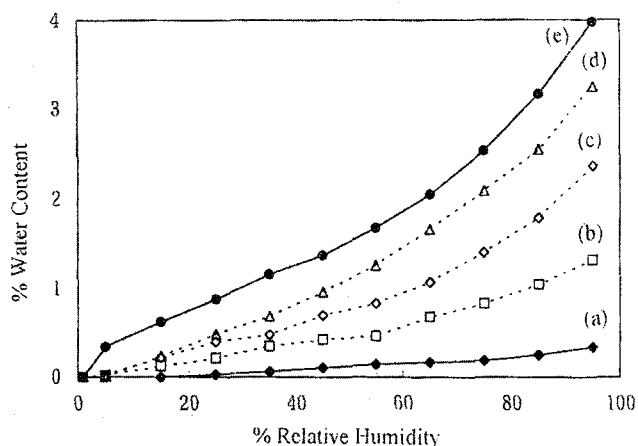


**Figure 4**—Water sorption isotherms of CS-891 with different crystallinity at 35°C. (◆) ICS100, (□) ICS70, (◇) ICS 50, (△) ICS30, (●) ICS0.

tion relative to ground CS-891. With a decrease of crystalline CS-891, the water sorption isotherm of amorphous CS-891 was increased, and this suggested that amorphous CS-891 was hygroscopic, so that the adsorbed water increased with an increase of amorphous CS-891.

#### Solubility and Dissolution Behaviors

Table II shows the solubilities of crystalline CS-891 and maximum concentration (apparent solubility) of each sample with different crystallinity in which the apparent solubility was not the true value because the transformation rate of the amorphous to the crystalline CS-891 was very high.<sup>17)</sup> The apparent solubility of ground CS-891 was 4.4  $\mu\text{g}/\text{ml}$  and the solubility of intact CS-891 was 3.1  $\mu\text{g}/\text{ml}$  at  $37\pm 1^\circ\text{C}$ . The apparent precipitation rates were decreased with an increase of mixture ratios of 10:0 (ICS100), 7:3 (ICS70), 5:5 (ICS50), 3:7 (ICS30) and 0:10 (ICS0) (intact:ground CS-891) (Figure 5, 6). The dissolution profile of intact and ground CS-891 at various stirring speed is shown in Figure 6, and the dissolution rate was increased with an increase of a stirring speed, and the precipitation rate of ground CS-891 was higher than that of intact CS-891. Figure 7 shows the initial dissolution profiles of ICS100, ICS70, ICS50, ICS30 and ICS0 at  $37\pm 1^\circ\text{C}$  by the USP paddle method. The apparent dissolution rate constants within 0-8 min. were obtained using the Higuchi model, which was for diffusion release given by Higuchi is  $100-M = kt^{1/2}$ , where  $M$  is the percent of drug undissolved,  $k$  is the dissolution rate constant, and  $t$  is the time of dissolution.<sup>19)</sup> Table II shows the apparent dissolution rate constants of ICS100, ICS70, ICS50, ICS30 and ICS0 were 0.451, 1.713, 2.054, 2.512, 2.657, and the apparent dissolution rate constant of ground CS-891 was about 5.9 fold higher than that of intact CS-891. After

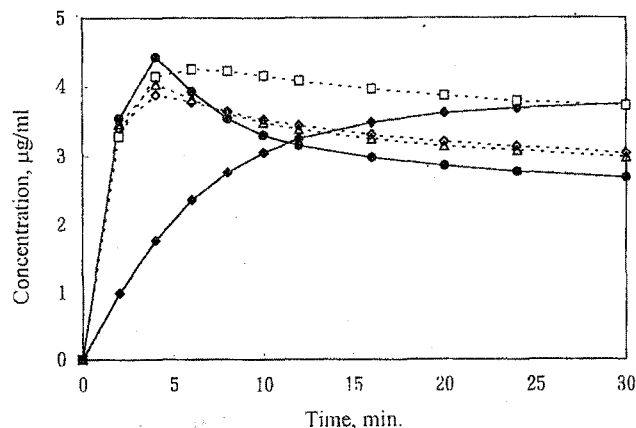


**Figure 5**—Apparent solubilities of ICS100, ICS70, ICS50, ICS30 and ICS0. (◆) ICS100, (□) ICS70, (◇) ICS 50, (△) ICS30, (●) ICS0.

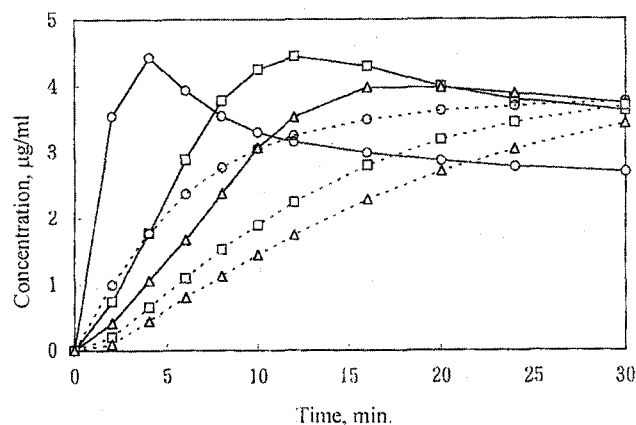


**Figure 6**—Effect of stirring speed on the dissolution profiles of intact (dotted line) and ground CS-891 (solid line) in supersaturated solution at 37°C. (○) 200 rpm, (□) 100 rpm, (△) 50 rpm.

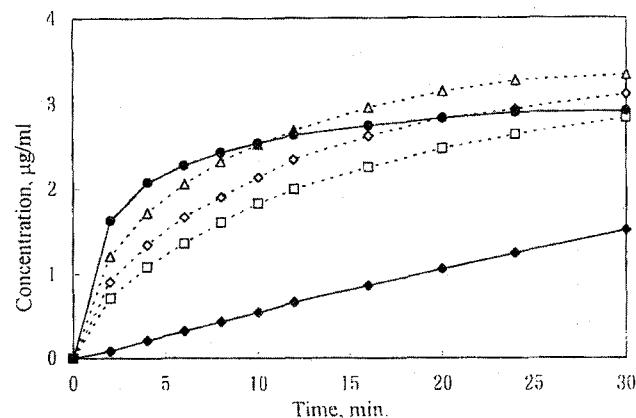


**Figure 7**—Dissolution profiles of ICS-891, ICS70, ICS50, ICS30 and ICS0 at 37°C by the USP paddle method. (◆) ICS100, (□) ICS70, (◇) ICS 50, (△) ICS30, (●) ICS0.

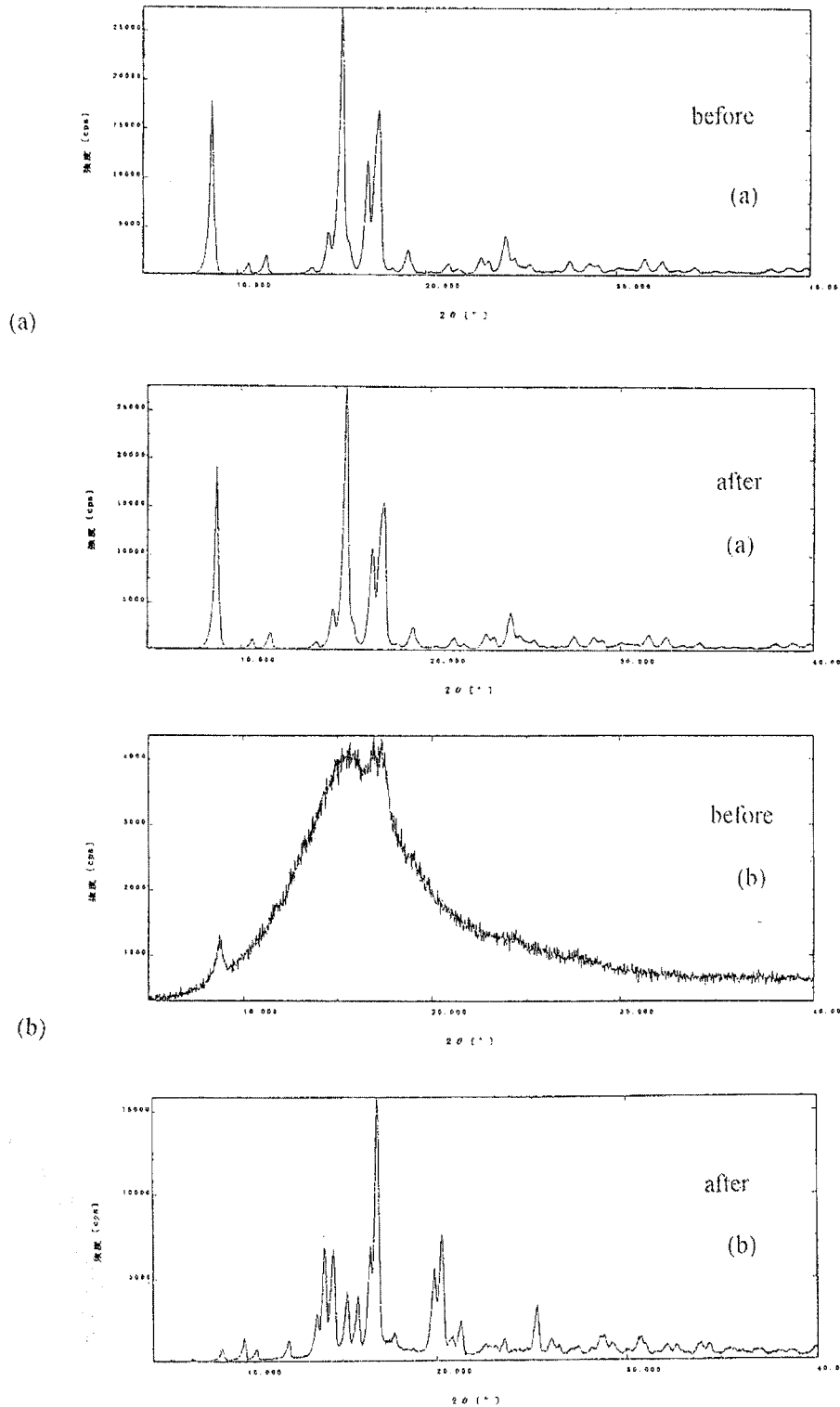


**Figure 8**—Powder X-ray diffraction profiles of intact and ground CS-891 before and after the solubility test. (a) intact CS-891, (b) ground CS-891.

the solubility experiment for intact and ground CS-891, described above, the crystallized precipitates in various solution were investigated using X-ray diffractometry and DSC

(Figure 8, 9). Changes in the powder XRD patterns of the crystallized precipitate after the solubility test were also shown in Figure 8. This might suggest the solid on the surface of CS-

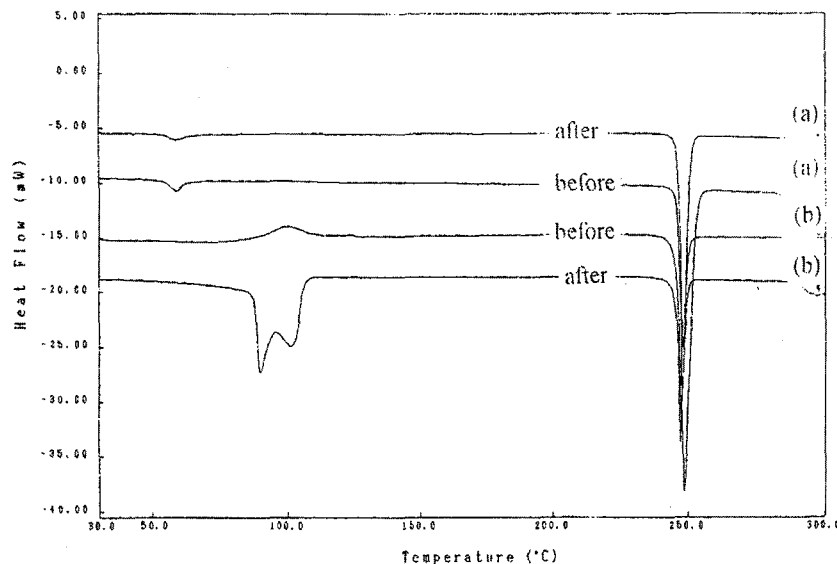


Figure 9—DSC thermograms of intact and ground CS-891 before and after the solubility test. (a) intact CS-891, (b) ground CS-891.

891 is transformed from amorphous form to a crystalline form during the solubility experiment.

### Conclusions

With increase of amorphous CS-891 in mixture ratios, the intensities of X-ray diffraction peaks of crystalline CS-891 were decreased but surface area, water absorption isotherm, and exothermic peaks in DSC were increased. The apparent solubility of ground CS-891 was about 1.4-fold higher than the solubility of intact CS-891 at  $37 \pm 1^\circ\text{C}$ , and the apparent dissolution rate constant of ground CS-891 was about 5.9-fold higher than that of intact CS-891. A good relationships were obtained between the crystallinity of CS-891 and apparent dissolution rate constant ( $r > 0.96$ ). A crystalline form of CS-891 transformed from amorphous CS-891 after the solubility test was found by X-ray diffraction analysis and DSC. It seems that the transformations between solid phase are a very important aspect in the development of a dosage form, since the bio-availability of its preparations are affected by the solubility and dissolution of bulk powder.

### References

- 1) G.H. Rasmusson, G.F. Reynolds, T. Utne, R.B. Jobson, R.L. Primka, C. Berman and J.R. Brooks, Azasteroids as inhibitor of rat prostatic  $5\alpha$ -reductase, *J. Med. Chem.*, **27**, 1690-1701 (1984).
- 2) T. Liang, M.A. Cascieri, A.H. Cheung, G.F. Reynolds and G.H. Rasmusson, Species differences in prostatic steroid  $5\alpha$ -reductases of rat, dog and human, *Endocrinology*, **117**, 571-579 (1985).
- 3) R. Brooks, C. Berman, R.L. Primka, G. Reynolds and G.H. Rasmusson,  $5\alpha$ -reductase inhibitory and antiandrogenic activities of some 4-azasteroids in the rat, *Steroids*, **47**, 1-19 (1986).
- 4) P.K. Siiteri and J.D. Wilson, Dihydrotestosterone in prostatic hypertrophy, *J. Clin. Invest.*, **49**, 1737-1745 (1970).
- 5) R.C. Rowe, A.G. McKillop and D. Bray, The effect of batch and source variation on the crystallinity of microcrystalline cellulose, *Int. J. Pharmaceut.*, **101**, 169-172 (1994).
- 6) M.L. Shively and S. Myers, Solid-state emulsions; the effect of process and storage conditions, *Pharm. Res.*, **10**, 1071 (1993).
- 7) M. Landin, R.M. Pacheco, J.L.G. Azoma, C. Souto, A. Concheiro and R.C. Rowe, Effect of country of origin on the properties of microcrystalline cellulose, *Int. J. Pharmaceut.*, **91**, 123-131 (1993).
- 8) K. Takeshima, N. Sunagawa, S. Nagata, K. Hirano and Y. Takagishi, Effect of morphological properties on drug release from biodegradable microspheres, *Yakugaku Zasshi*, **112**, 203-210 (1992).
- 9) T. Yamaguchi, M. Nishimura, R. Okamoto, T. Takeuchi and K. Yamamoto, Glass formation of 4''-O-(4-methoxyphenyl) acetyltalosin and physicochemical stability of the amorphous solid, *Int. J. Pharmaceut.*, **85**, 87-96 (1992).
- 10) Y. Nakai, K. Yamamoto, K. Terada and A. Kajiyama, Relationship between crystallinity of  $\beta$ -cyclodextrin and tablet characteristics, *Chem. Pharm. Bull.*, **33**, 5110-5112 (1985).
- 11) M. Morita, Y. Nakai, E. Fukuka and S. Nakajima, Physicochemical properties of crystalline lactose, *Chem. Pharm. Bull.*, **32**, 4076-4083 (1984).
- 12) Y. Nakai, K. Yamamoto and K. Terada, Crystallinity changes of  $\alpha$ - and  $\beta$ -cyclodextrins by grinding, *Yakugaku Zasshi*, **105**, 580-585 (1985).

- 13) Y. Nakai, K. Yamamoto, K. Terada and K. Akimoto, The dispersed states of medicinal molecules in ground mixtures with  $\alpha$ - and  $\beta$ -cyclodextrin, *Chem. Pharm. Bull.*, **32**, 685-691 (1984).
- 14) S. Lowell, Continuous flow krypton adsorption for flow surface area measurements, *Anal. Chem.*, **45**, 1576-1577 (1973).
- 15) L.J.M. Tasic, M.D. Jovanovic and Z.R. Djuric, The influence of  $\beta$ -cyclodextrin on the solubility and dissolution rate of paracetamol solid dispersion, *J. Pharm. Pharmacol.*, **44**, 52-55 (1992).
- 16) M. Otsuka and N. Kaneniwa, Solubility of cephalixin crystals, *Yakugaku Zasshi*, **102**, 967-971 (1982).
- 17) M. Otsuka, R. Teraoka and Y. Matsuda, Physicochemical properties of nitrofurantoin anhydrate and monohydrate and their dissolution, *Chem. Pharm. Bull.*, **39**, 2667-2670 (1991).
- 18) P.H. Hermans and A. Weidinger, Quantitative X-ray investigation on the crystallinity of cellulose fiber a background analysis, *J. Appl. Phys.*, **19**, 491-506 (1948).
- 19) T. Higuchi, mechanism of sustained-action medication, *J. Pharm. Sci.*, **52**, 1145-1149 (1963).